

Post-Regularization Confidence Bands for Ordinary Differential Equations

XIAOWU DAI AND LEXIN LI

University of California at Berkeley

Abstract

Ordinary differential equation (ODE) is an important tool to study the dynamics of a system of biological and physical processes. A central question in ODE modeling is to infer the significance of individual regulatory effect of one signal variable on another. However, building confidence band for ODE with unknown regulatory relations is challenging, and it remains largely an open question. In this article, we construct post-regularization confidence band for individual regulatory function in ODE with unknown functionals and noisy data observations. Our proposal is the first of its kind, and is built on two novel ingredients. The first is a new localized kernel learning approach that combines reproducing kernel learning with local Taylor approximation, and the second is a new de-biasing method that tackles infinite-dimensional functionals and additional measurement errors. We show that the constructed confidence band has the desired asymptotic coverage probability, and the recovered regulatory network approaches the truth with probability tending to one. We establish the theoretical properties when the number of variables in the system can be either smaller or larger than the number of sampling time points, and we study the regime-switching phenomenon. We demonstrate the efficacy of the proposed method through both simulations and illustrations with two data applications.

Key Words: De-biasing; Local polynomial approximation; Ordinary differential equations; Reproducing kernel Hilbert space; Smoothing spline analysis of variance.

1 Introduction

Characterizing the dynamics of biological and physical processes is of fundamental interest in a large variety of scientific fields, and ordinary differential equation (ODE) is a frequently used tool to address such type of problems. Examples include infectious disease (Liang and Wu, 2008), genomics (Cao and Zhao, 2008; Ma et al., 2009; Wu et al., 2014), neuroscience (Izhikevich, 2007; Zhang et al., 2015a, 2017; Cao et al., 2019), among many others. An ODE system models the changes of a set of variables of interest, quantified by their derivatives with respect to time, as functions of all other variables in the system. Typically, the system is observed on discrete time points with some additive measurement errors. In recent years, there has been an increased number of proposals for ODE modeling. One family of ODE models adopt linear functional forms in the ODE system; for instance, Lu et al. (2011) proposed a set of linear ODEs, Zhang et al. (2015a) extended to include two-way interactions, and Dattner and Klaassen (2015) further extended to a generalized linear form using a finite set of known basis functions. Another family of ODE models consider additive functionals; for instance, Henderson and Michailidis (2014); Wu et al. (2014); Chen et al. (2017) proposed the generalized additive model with a set of common basis functions plus an unknown residual function. The third family studies the ODE system when the functional forms are completely known (González et al., 2014; Zhang et al., 2015b; Mikkelsen and Hansen, 2017). Recently, Dai and Li (2021) proposed reproducing kernel-based ODEs to flexibly model the unknown functionals of both main effects and two-way interactions.

A central question in ODE modeling is about *inference* of significance of individual regulatory relations among the variables in the system (Ma et al., 2009). The majority of existing ODE solutions have been focusing on regularized sparse *estimation* of the ODEs. Even though sparse estimation can in effect identify such relations, it does not produce a quantification of statistical significance explicitly, nor controls the false discovery explic-

itly. In general, inference is an utterly different problem from sparse estimation. When the functional forms are completely *known* in an ODE system, confidence intervals for the ODE parameters have been studied and been mostly built upon asymptotic normality of finite-dimensional parameters (Ramsay et al., 2007; Miao et al., 2014; Zhang et al., 2015b; Wu et al., 2019). When the functional forms are *unknown*, however, there is *no* existing solution for individual ODE parameter inference. Dai and Li (2021) derived the confidence interval of the entire signal trajectory in kernel ODEs with unknown functionals. Nevertheless, their method could *not* infer the *individual* regulatory effect of one variable on another, but instead only the *sum* of all individual effects. Building confidence intervals for individual ODE parameters with unknown regulatory relations is particularly challenging, as it involves infinite-dimensional functionals. There is a clear gap in the current literature on ODE inference.

In this article, we tackle the ODE inference problem with unknown functionals and noisy data observations. Our goal is to directly construct the confidence band for any individual regulatory functional that measures the effect of one signal variable on another. The constructed confidence band provides both an uncertainty quantification for the individual regulatory relation, and also a sparse recovery of the entire regulatory system when coupled with a proper FDR control. We establish the confidence band for both low-dimensional and high-dimensional settings, where the number of variables in the system can be smaller or larger than the number of sampling time points, and we study the regime-switching phenomenon. We show that the constructed confidence band has the desired asymptotic coverage probability, and the recovered regulatory network approaches the truth with probability tending to one. Toward our goal, we propose and develop two novel methodological and technical ingredients: a new *localized kernel learning* approach that combines reproducing kernel learning with local Taylor approximation, and a new debiasing method that tackles infinite-dimensional functionals and additional measurement errors. Consequently, our proposal makes useful contributions on multiple fronts, includ-

ing ODE estimation and inference, nonparametric modeling, as well as high-dimensional inference with measurement errors.

The first component is a new localized kernel learning approach that in effect fuses two widely used nonparametric modeling techniques, reproducing kernel learning methods (Wahba, 1990), and local polynomial methods (Fan and Gijbels, 1996). More specifically, we adopt the kernel ODE model of Dai and Li (2021), which is built upon the learning framework of reproducing kernel Hilbert space (RKHS, Aronszajn, 1950; Wahba, 1990) and smoothing spline analysis of variance (SS-ANOVA, Wahba et al., 1995; Huang, 1998; Lin and Zhang, 2006). This model allows highly flexible and unknown forms for the functions in the ODE system as well as interactions. Meanwhile, we employ the Taylor expansion and local approximation idea, which is frequently employed in local polynomial nonparametric regressions (Fan and Gijbels, 1996; Opsomer and Ruppert, 1997). Such a fused method essentially characterizes the regulatory effect of one variable on another in the ODE system through a scalar quantity, which in turn allows us to derive the corresponding confidence band. Moreover, this localized kernel learning approach is potentially useful for other nonparametric modeling problems beyond ODEs.

We remark that our method is related to but also substantially different from the kernel ODE method of Dai and Li (2021), and the kernel-sieve hybrid method of Lu et al. (2020). Compared to Dai and Li (2021), although we adopt the same ODE model framework, our estimator is utterly different after introducing the local approximation. Actually, our localized kernel estimator has a slower convergence rate compared to the minimax rate of the estimator of Dai and Li (2021) in a low-dimensional setting; see Section 5.1. On the other hand, this slower rate is sufficient for constructing an asymptotically valid confidence band. More importantly, the method of Dai and Li (2021) can only obtain the confidence interval for the entire signal trajectory, which is the *sum* of *all* individual effects, but not for a *single* individual effect of one variable on another. Directly adopting the estimator of Dai and Li (2021) can *not* obtain the individual confidence band we target. Compared to

Lu et al. (2020) who tackled the inference problem of a nonparametric additive model, our ODE inference method differs in multiple ways, including that the signals are not directly observed but need to be estimated from the data with error, there are pairwise interaction terms, and the ODE estimation involves integrals. These differences have introduced a whole new set of challenges than Lu et al. (2020), and thus an utterly different solution.

We also remark that, by choosing a proper linear kernel or additive kernel, the kernel ODE model includes the linear ODE (Zhang et al., 2015a) and the additive ODE (Chen et al., 2017) as special cases. Consequently, our inference solution is applicable to a range of different ODE models. Our work thus addresses a scientific question that is crucial but currently still remains open, and makes a useful addition to the ODE toolbox.

The second component is a new de-biasing method for the localized kernel ODE estimator. We observe that the individual regulatory effects in ODE models are nonparametric functionals, which are estimated through proper regularizations in terms of the RKHS norms. De-biasing is an important tool to perform post-regularization high-dimensional statistical inference (Zhang and Zhang, 2014; van de Geer et al., 2014; Ning and Liu, 2017; Zhang and Cheng, 2017). However, in ODEs, the signal variables themselves are not directly observed, but only their noisy counterparts, and they need to be estimated given the noisy data. Besides, the objects of inference are infinite-dimensional functionals, and their estimation involves integrals. These extra layers of complications have introduced new difficulties for de-biasing. To overcome those difficulties, we introduce a new bias correction score with integral of the estimated functional. We also generalize Chernozhukov et al. (2014) and perform a new approximation analysis for the Gaussian multiplier bootstrap within the RKHS framework. Our method is the first de-biasing solution for ODE models, and thus also contributes to the literature on de-biasing. In addition, it is potentially useful for high-dimensional inference of other statistical models that involve latent variables and measurement errors (Wansbeek and Meijer, 2001).

The rest of the article is organized as follows. Section 2 first introduces the kernel

ODE model, then develops the localized kernel learning approach. Section 3 presents the parameter estimation, and Section 4 derives the confidence band formula. Section 5 establishes the convergence rate and coverage property of the proposed method. Section 6 investigates the finite-sample performance, and Section 7 illustrates with two real data examples. The Supplementary Appendix collects all technical proofs.

2 Localized Kernel Learning for ODE

In this section, we first present the kernel ODE model, then propose the localized kernel learning method, which fuses reproducing kernel learning and local polynomial approximation, and is crucial for subsequent ODE inference.

2.1 Kernel ODE model

Let $x(t) = (x_1(t), \dots, x_p(t))^\top \in \mathbb{R}^p$ denote the set of p variables of interest, and t index the time in a standardized interval $\mathcal{T} = [0, 1]$. We consider the ODE system,

$$\frac{dx(t)}{dt} = \begin{pmatrix} \frac{dx_1(t)}{dt} \\ \vdots \\ \frac{dx_p(t)}{dt} \end{pmatrix} = \begin{pmatrix} F_1(x(t)) \\ \vdots \\ F_p(x(t)) \end{pmatrix} = F(x(t)), \quad (1)$$

where $F = \{F_1, \dots, F_p\}$ denotes the set of unknown functionals that characterize the regulatory relations among $x(t)$. Typically, the system (1) is observed on a set of n discrete time points $\{t_1, \dots, t_n\}$, with additional measurement errors,

$$y_i = x(t_i) + \epsilon_i, \quad i = 1, \dots, n, \quad (2)$$

where $y_i = (y_{i1}, \dots, y_{ip})^\top \in \mathbb{R}^p$ denotes the observed data, and $\epsilon_i = (\epsilon_{i1}, \dots, \epsilon_{ip})^\top \in \mathbb{R}^p$ denotes the vector of measurement errors that are usually assumed to follow an independent normal distribution with mean 0 and variance σ_j^2 , $j = 1, \dots, p$. Besides, the system (1) usually starts with an initial condition $x(0) \in \mathbb{R}^p$.

In a biological and physical system, given the observed noisy time-course data $\{y_i\}_{i=1}^n$, a central question of interest is to uncover the structure of the system of ODEs in terms of which variables regulate which other variables. We say that $x_k(t)$ regulates $x_j(t)$, if F_j is a non-zero functional of $x_k(t)$. That is, $x_k(t)$ affects $x_j(t)$ through the functional F_j on its derivative $dx_j(t)/dt$, for $j, k = 1, \dots, p$. We consider the following model for F_j ,

$$F_j(x(t)) = \theta_{j0} + \sum_{l=1}^p F_{jl}(x_l(t)) + \sum_{l=1, l \neq r}^p \sum_{r=1}^p F_{jlr}(x_l(t), x_r(t)), \quad j = 1, \dots, p, \quad (3)$$

where $\theta_{j0} \in \mathbb{R}$ denotes the global intercept, F_{jl} and F_{jlr} denote the main effect and two-way interaction, respectively. Higher-order interactions are possible, but two-way interactions are most common in ODEs (Ma et al., 2009; Zhang et al., 2015a).

We adopt the kernel ODE model of Dai and Li (2021) for (3), and build the model within the smoothing spline ANOVA framework (Wahba et al., 1995; Gu, 2013; Lin and Zhang, 2006). Specifically, let \mathcal{H}_l denote a space of functions of $x_l(t) \in \mathcal{X}$ with zero marginal integral, where $\mathcal{X} \subset \mathbb{R}$ is a compact set. Let $\{1\}$ denote the space of constant functions. Construct the tensor product space as

$$\mathcal{H} = \{1\} \oplus \sum_{l=1}^p \mathcal{H}_l \oplus \sum_{l=1, l \neq r}^p \sum_{r=1}^p (\mathcal{H}_l \otimes \mathcal{H}_r). \quad (4)$$

We assume the functionals F_j , $j = 1, \dots, p$, in the ODE model (3) are located in the space of \mathcal{H} . The identifiability of the terms in (3) is assured by the conditions specified through the averaging operator: $\int_{\mathcal{T}} F_{jl}(x_l(t)) dt = 0$, for $l = 1, \dots, p$.

2.2 Localized kernel learning

Our primary goal is to infer the individual regulatory effect of $x_k(t)$ on $x_j(t)$, for a given pair of $j, k = 1, \dots, p$, in the ODE system (1). Next, we introduce the Tayler expansion and local approximation idea into our kernel ODE model framework. In effect, we fuse two perhaps most popular nonparametric modeling techniques, reproducing kernel learning methods (Wahba, 1990) and local polynomial methods (Fan and Gijbels, 1996).

We observe that the regulatory effect of $x_k(t)$ on a given $x_j(t)$ is encoded in two parts: the main effect term, $F_{jk}(x_k(t))$, $j, k = 1, \dots, p$, and the two-way interaction terms, $F_{jkl}(x_k(t), x_l(t))$, $l = 1, \dots, p, l \neq k$. We next study the two parts separately.

For the main effect term $F_{jk}(x_k(t))$, consider the Taylor expansion at a fixed time point $t = t_0$. Letting \tilde{t} be a point locating between t_0 and t , by the chain rule, we have,

$$F_{jk}(x_k(t)) = F_{jk}(x_k(t_0)) + \frac{dF_{jk}(x_k(\tilde{t}))}{dx_k} \frac{dx_k(\tilde{t})}{dt} (t - t_0).$$

Since $F_{jk}(x_k(t_0))$ is a constant at the fixed t_0 and does not vary with t , we denote $F_{jk}(x_k(t_0)) \equiv \alpha_{jk,t_0}$. Besides, suppose that both functions $F_{jk}(\cdot)$ and $x_k(\cdot)$ are in some RKHS that have continuous first derivatives, then $dF_{jk}(x_k(t))/dx_k$ and $dx_k(t)/dt$ are continuous functions in t . Henceforth, when $t \rightarrow t_0$, the second term in the above Taylor expansion goes to zero. Thus we can approximate $F_{jk}(x_k(t))$ by α_{jk,t_0} . Moreover, the rest of the main effect terms $F_{jl}(x_l(t))$, $l = 1, \dots, p, l \neq k$, can be viewed as nuisance parameters when inferring the effect of $x_k(t)$ on $x_j(t)$.

For the interaction terms $F_{jkl}(x_k(t), x_l(t))$, $l = 1, \dots, p, l \neq k$, since $\{1\} \otimes \mathcal{H}_l = \mathcal{H}_l$ (Wahba, 1990), $F_{jkl}(x_k(t), x_l(t))$ is absorbed into the main effect term $F_{jk}(x_k(t))$ when $F_{jk}(x_k(t))$ is approximated by the constant α_{jk,t_0} . In other words, when the effect of $x_k(t)$ on $x_j(t)$ holds constant, then the change of the joint effect of $(x_k(t), x_l(t))$ on $x_j(t)$ only depends on the change of the effect of $x_k(t)$ on $x_j(t)$. Another way to see this is that, since $F_{jkl} \in \mathcal{H}_k \otimes \mathcal{H}_l$ in (4), there exists a finite integer s , such that

$$F_{jkl} = \sum_{\nu=1}^s F_{jk\nu} F_{j\nu l} = \sum_{\nu=1}^s \alpha_{jk,t_0} F_{j\nu l} = \alpha_{jk,t_0} \left(\sum_{\nu=1}^s F_{j\nu l} \right) \in \mathcal{H}_l,$$

where the second equality is due to $F_{jk\nu}(x_k(t)) = \alpha_{jk,t_0}$ as $t \rightarrow t_0$, and $F_{j\nu l} \in \mathcal{H}_l$.

Together, following the Taylor approximation that $F_{jk}(x_k(t)) = \alpha_{jk,t_0}$ as $t \rightarrow t_0$, the regulatory effect of $x_k(t)$ on $x_j(t)$ is captured by the scalar α_{jk,t_0} . Consequently, we can build a confidence band based on α_{jk,t_0} to infer the effect of $x_k(t)$ on $x_j(t)$. Moreover, the identifiability of the terms in (3) implies that α_{jk,t_0} should satisfy $\int_{\mathcal{T}} \alpha_{jk,t_0} dt_0 = 0$. In our

implementation, we sample a sequence of time points in $\mathcal{T} = [0, 1]$ as t_0 , then centralize α_{jk,t_0} by subtracting the average.

Next, we estimate α_{jk,t_0} at any given time point $t_0 \in \mathcal{T}$, along with other nuisance terms in F_j , through the localized estimation (Fan and Gijbels, 1996). Specifically, write $F_j = \theta_{j0} + \tilde{F}_j$, where θ_{j0} is the global mean, and \tilde{F}_j is the centralized functional, $j = 1, \dots, p$. If t is at the local neighborhood of t_0 , we write

$$\begin{aligned}\tilde{F}_j(x(t)) &= \alpha_{jk,t_0} + \sum_{l=1, l \neq k}^p F_{jl}(x_l(t)) + \sum_{l=1, l \neq k, r}^p \sum_{r=1, r \neq k}^p F_{jlr}(x_l(t), x_r(t)) \\ &\equiv \alpha_{jk,t_0} + H_j(x(t)),\end{aligned}\tag{5}$$

where H_j collects all the nuisance components when evaluating the effect of $x_k(t)$ on $x_j(t)$.

We next develop a procedure to estimate θ_{j0} and \tilde{F}_j in (5).

3 ODE Estimation

In this section, we develop an estimation procedure, where we adopt a two-step collocation approach (Varah, 1982). We first estimate model (3) under the constraint that $F_j \in \mathcal{H}$ in (4), then incorporate the local approximation in (5). Next, we derive the corresponding optimization algorithm to estimate the unknown parameters.

3.1 Two-step collocation estimation

We adopt the two-step collocation method that is commonly used in ODE estimation.

The first step is to obtain a smoothing spline estimate $\hat{x}(t) = (\hat{x}_1(t), \dots, \hat{x}_p(t))^\top$,

$$\hat{x}_j(t) = \arg \min_{z_j \in \mathcal{F}} \left\{ \frac{1}{n} \sum_{i=1}^n [y_{ij} - z_j(t_i)]^2 + \lambda_{nj} \|z_j(t)\|_{\mathcal{F}}^2 \right\}, \quad j = 1, \dots, p,\tag{6}$$

where \mathcal{F} is the function space where $x_j(t)$ reside in, and does not have to be the same as \mathcal{H} , $\|\cdot\|_{\mathcal{F}}$ is the norm of \mathcal{F} , z_j is a function in \mathcal{F} that we minimize over, and λ_{nj} is the smoothness parameter that is often tuned by generalized cross-validation (Wahba, 1990).

The second step is to estimate $F_j = \theta_{j0} + \tilde{F}_j$. We solve the penalized optimization,

$$\min_{\theta_{j0}, \tilde{F}_j} \left\{ \frac{1}{n} \sum_{i=1}^n \left[y_{ij} - \theta_{j0} - \int_0^{t_i} \tilde{F}_j(\hat{x}(t)) dt \right]^2 + \tau_{nj} \left(\sum_{l=1}^p \|\mathcal{P}^l \tilde{F}_j\|_{\mathcal{H}} + \sum_{l=1, l \neq r}^p \sum_{r=1}^p \|\mathcal{P}^{lr} \tilde{F}_j\|_{\mathcal{H}} \right) \right\}, \quad (7)$$

where $\|\cdot\|_{\mathcal{H}}$ is the norm of \mathcal{H} , $\mathcal{P}^l \tilde{F}_j$ and $\mathcal{P}^{lr} \tilde{F}_j$ are the orthogonal projections of \tilde{F}_j , or equivalently F_j , onto \mathcal{H}_l and $\mathcal{H}_l \otimes \mathcal{H}_r$, respectively, and τ_{nj} is the penalty parameter. Note that the optimization problem (7) deals with the integral $\int_0^{t_i} \tilde{F}_j(\hat{x}(u)) du$, rather than the derivative $d\hat{x}_j(t)/dt$. This follows a similar spirit as Dattner and Klaassen (2015), and is to produce a more robust estimate. Moreover, the penalty function in (7) is a sum of RKHS norms on the main effects and pairwise interactions, which is similar in spirit as the component selection and smoothing operator penalty of Lin and Zhang (2006).

To solve (7), we first obtain an estimator of the global mean θ_{j0} in F_j as

$$\hat{\theta}_{j0} = \bar{y}_j - \int_{\mathcal{T}} \bar{T}(t) \tilde{F}_j(\hat{x}(t)) dt, \quad (8)$$

where $\bar{y}_j = n^{-1} \sum_{i=1}^n y_{ij}$, $\bar{T}(t) = n^{-1} \sum_{i=1}^n T_i(t)$, $T_i(t) = \mathbb{I}\{0 \leq t \leq t_i\}$, and $\mathbb{I}(\cdot)$ is the indicator function. We then estimate the centralized component \tilde{F}_j in F_j by plugging (8) into (7), and solving the penalized optimization,

$$\min_{\tilde{F}_j \in \mathcal{H}} \left\{ \frac{1}{n} \sum_{i=1}^n \left[(y_{ij} - \bar{y}_j) - \int_{\mathcal{T}} (T_i(t) - \bar{T}(t)) \tilde{F}_j(\hat{x}(t)) dt \right]^2 + \tau_{nj} \left(\sum_{k=1}^p \|\mathcal{P}^k \tilde{F}_j\|_{\mathcal{H}} + \sum_{k=1, k \neq l}^p \sum_{l=1}^p \|\mathcal{P}^{kl} \tilde{F}_j\|_{\mathcal{H}} \right) \right\}. \quad (9)$$

Next, we introduce the localization as specified in (5). Let $R : \mathcal{T} \mapsto \mathbb{R}$ be a symmetric density function with a bounded support. Denote $R_h(\cdot) = h^{-1} R(\cdot/h)$, where $h > 0$ is the bandwidth. Following (5) and (9), we estimate $\alpha_{jk, t_0} \in \mathbb{R}$ and $H_j \in \mathcal{H}$ through the localized and penalized optimization,

$$\min_{\alpha_{jk, t_0}, H_j} \left\{ \frac{1}{n} \sum_{i=1}^n R_h(t_i - t_0) \left[(y_{ij} - \bar{y}_j) - \alpha_{jk, t_0} \bar{t}_i - \int_{\mathcal{T}} (T_i(t) - \bar{T}(t)) H_j(\hat{x}(t)) dt \right]^2 + \tau_{nj} \left(\sum_{l=1, l \neq k}^p \|\mathcal{P}^l H_j\|_{\mathcal{H}} + \sum_{l=1, l \neq k, r}^p \sum_{r=1, r \neq k}^p \|\mathcal{P}^{lr} H_j\|_{\mathcal{H}} \right) \right\}, \quad (10)$$

where $\bar{t}_i = t_i - n^{-1} \sum_{i=1}^n t_i$. The estimate $\hat{\alpha}_{jk,t_0}$ obtained from (10) captures the individual regulatory effect of $x_k(t)$ on $x_j(t)$ in a local neighborhood of $t_0 \in \mathcal{T}$.

Now, given the estimates $\hat{x}_j(t)$ from (6), $\hat{\theta}_{j0}$ from (8), and $\hat{\alpha}_{jk,t_0}, \hat{H}_j$ from (10), we estimate the p -dimensional functional $F_j(x(t_0)) = \theta_{j0} + F_{jk}(x_k(t_0)) + \sum_{l=1, l \neq k}^p F_{jl}(x_l(t_0)) + \sum_{l=1, l \neq r}^p \sum_{r=1}^p F_{jlr}(x_l(t_0), x_r(t_0))$ at any time point $t_0 \in \mathcal{T}$ by

$$\hat{F}_j(\hat{x}(t_0)) = \hat{\theta}_{j0} + \hat{\alpha}_{jk,t_0} + \hat{H}_j(\hat{x}(t_0)), \quad j = 1, \dots, p. \quad (11)$$

We comment that, due to the Taylor approximation and localization, our localized kernel ODE estimator in (11) is different from the kernel ODE estimator of Dai and Li (2021) obtained from (7). In Section 5.1, we study its convergence rate, and compare it to the minimax optimal rate of the kernel ODE estimator of Dai and Li (2021).

3.2 Optimization algorithm

We next develop an optimization algorithm to solve (10). This algorithm has a similar overall structure as that of Dai and Li (2021). Nevertheless, it differs in that a local weight R_h is introduced, and the estimations of the parameter of interest α_{jk,t_0} and the rest of nuisance parameters are separated. Specifically, we consider the following optimization problem that is equivalent to (10),

$$\begin{aligned} \min_{\theta_j, \alpha_{jk,t_0}, H_j} & \left\{ \frac{1}{n} \sum_{i=1}^n R_h(t_i - t_0) \left[(y_{ij} - \bar{y}_j) - \alpha_{jk,t_0} \bar{t}_i - \int_{\mathcal{T}} (T_i(t) - \bar{T}(t)) H_j(\hat{x}(t)) dt \right]^2 \right. \\ & + \eta_{nj} \left(\sum_{l=1, l \neq k}^p \theta_{jl}^{-1} \|\mathcal{P}^l H_j\|_{\mathcal{H}}^2 + \sum_{l=1, l \neq k}^p \sum_{r=1, r \neq l, k}^p \theta_{jlr}^{-1} \|\mathcal{P}^{lr} H_j\|_{\mathcal{H}}^2 \right) \\ & \left. + \kappa_{nj} \left(\sum_{l=1, l \neq k}^p \theta_{jl} + \sum_{l=1, l \neq k}^p \sum_{r=1, r \neq l, k}^p \theta_{jlr} \right) \right\}, \end{aligned} \quad (12)$$

subject to $\theta_j \geq 0$, where $\theta_j = \{\theta_{jl}\}_{l \neq k} \cup \{\theta_{jlr}\}_{l \neq k; r \neq l, k} \in \mathbb{R}^{(p-1)^2}$ collects all the parameters to estimate, and $\eta_{nj}, \kappa_{nj} \geq 0$ are the tuning parameters, $j = 1, \dots, p$. The two optimizations (10) and (12) are equivalent in the sense that, if $(\hat{\alpha}_{jk,t_0}, \hat{H}_j)$ minimizes (10), then $(\hat{\theta}_j, \hat{\alpha}_{jk,t_0}, \hat{H}_j)$ minimizes (12), with $\hat{\theta}_{jl} = \eta_{nj}^{1/2} \kappa_{nj}^{-1/2} \|\mathcal{P}^l \hat{H}_j\|_{\mathcal{H}}$, and $\hat{\theta}_{jlr} =$

$\eta_{nj}^{1/2} \kappa_{nj}^{-1/2} \|\mathcal{P}^{lr} \hat{H}_j\|_{\mathcal{H}}$, $l, r = 1, \dots, p$, $l, r \neq k$, $l \neq r$. Meanwhile, if $(\hat{\theta}_j, \hat{\alpha}_{jk,t_0}, \hat{H}_j)$ minimizes (12), then $(\hat{\alpha}_{jk,t_0}, \hat{H}_j)$ minimizes (10).

Next, we develop an iterative alternating procedure to solve (12), by first estimating (α_{jk,t_0}, H_j) given θ_j , then estimating θ_j given (α_{jk,t_0}, H_j) .

For a given estimate $\hat{\theta}_j$, the optimization problem (12) becomes,

$$\min_{\alpha_{jk,t_0}, H_j} \left\{ \frac{1}{n} \sum_{i=1}^n R_h(t_i - t_0) \left[(y_{ij} - \bar{y}_j) - \alpha_{jk,t_0} \bar{t}_i - \int_{\mathcal{T}} (T_i(t) - \bar{T}(t)) H_j(\hat{x}(t)) dt \right]^2 \right. \\ \left. + \eta_{nj} \left(\sum_{l=1, l \neq k}^p \hat{\theta}_{jl}^{-1} \|\mathcal{P}^l H_j\|_{\mathcal{H}}^2 + \sum_{l=1, l \neq k}^p \sum_{r=1, r \neq l, k}^p \hat{\theta}_{jlr}^{-1} \|\mathcal{P}^{lr} H_j\|_{\mathcal{H}}^2 \right) \right\}. \quad (13)$$

Let $K_l(\cdot, \cdot) : \mathcal{X} \times \mathcal{X} \mapsto \mathbb{R}$ denote the kernel generating the RKHS \mathcal{H}_l , $l \neq k$. Then $K_{lr} = K_l K_r$ is the reproducing kernel of the RKHS $\mathcal{H}_l \otimes \mathcal{H}_r$ (Aronszajn, 1950). Let $K_{\theta_j} = \sum_{l=1, l \neq k}^p \hat{\theta}_{jl} K_l + \sum_{l=1, l \neq k}^p \sum_{r=1, r \neq l, k}^p \hat{\theta}_{jlr} K_{lr}$. By the representer theorem (Wahba, 1990), the solution \hat{H}_j to (13) is of the form,

$$\hat{H}_j(\hat{x}(t)) = \sum_{i=1}^n c_{ij} \int_{\mathcal{T}} K_{\theta_j}(\hat{x}(t), \hat{x}(s)) (T_i(s) - \bar{T}(s)) ds \quad (14)$$

for some $c_j = (c_{1j}, \dots, c_{nj})^\top \in \mathbb{R}^n$. Define two $n \times n$ matrices,

$$\Sigma = (\Sigma_{ii'}) \in \mathbb{R}^{n \times n}, \Sigma_{ii'} = \int_{\mathcal{T}} \int_{\mathcal{T}} \{T_i(s) - \bar{T}(s)\} K_{\theta_j}(\hat{x}(t), \hat{x}(s)) \{T_{i'}(t) - \bar{T}(t)\} ds dt, \quad (15)$$

$$R_{t_0} = \text{diag}\{R_h(t_1 - t_0), \dots, R_h(t_n - t_0)\} \in \mathbb{R}^{n \times n}.$$

Write $y_j = (y_{1j}, \dots, y_{nj})^\top \in \mathbb{R}^n$. Plugging (14) into (13), we reach the following weighted quadratic minimization problem in terms of $\{\alpha_{jk,t_0}, c_j\}$,

$$\min_{\alpha_{jk,t_0}, c_j} \left\{ \frac{1}{n} [(y_j - \bar{y}_j) - \alpha_{jk,t_0} \bar{t} - \Sigma c_j]^\top R_{t_0} [(y_j - \bar{y}_j) - \alpha_{jk,t_0} \bar{t} - \Sigma c_j] + \eta_{nj} c_j^\top \Sigma c_j \right\}, \quad (16)$$

where $\bar{t} = (\bar{t}_1, \dots, \bar{t}_n)^\top \in \mathbb{R}^n$. The optimization problem (16) has a closed-form solution; see Dai and Li (2021). The tuning parameter $\eta_{nj} \geq 0$ is selected by GCV (Wahba, 1990).

For a given estimate (α_{jk,t_0}, H_j) , the optimization problem (12) becomes,

$$\min_{\theta_j} \left\{ \frac{1}{n} (z_j - G\theta_j)^\top R_{t_0} (z_j - G\theta_j) + \kappa_{nj} \left(\sum_{l=1, l \neq k}^p \theta_{jl} + \sum_{l=1, l \neq k}^p \sum_{r=1, r \neq l, k}^p \theta_{jlr} \right) \right\}, \quad (17)$$

subject to $\theta_{jl} \geq 0, \theta_{jlr} \geq 0$, where the “response” is $z_j = (y_j - \bar{y}_j) - \hat{\alpha}_{jk,t_0}\bar{t} - (1/2)n\eta_{nj}c_j$, the “predictor” is $G \in \mathbb{R}^{n \times (p-1)^2}$, whose first $(p-1)$ columns are $\Sigma^l c_j$ with $l = 1, \dots, k-1, k+1, \dots, p$, and the last $(p-1)(p-2)$ columns are $\Sigma^{lr} c_j$ with $l, r = 1, \dots, k-1, k+1, \dots, p, l \neq r$, and $\Sigma^l = (\Sigma_{ii'}^l), \Sigma^{lr} = (\Sigma_{ii'}^{lr})$ are both $n \times n$ matrices whose (i, i') th entries are $\Sigma_{ii'}^l = \int_{\mathcal{T}} \int_{\mathcal{T}} \{T_i(s) - \bar{T}(s)\} K_l(\hat{x}(t), \hat{x}(s)) \{T_{i'}(t) - \bar{T}(t)\} ds dt$, and $\Sigma_{ii'}^{lr} = \int_{\mathcal{T}} \int_{\mathcal{T}} \{T_i(s) - \bar{T}(s)\} K_{lr}(\hat{x}(t), \hat{x}(s)) \{T_{i'}(t) - \bar{T}(t)\} ds dt$, respectively, where $i, i' = 1, \dots, n, j = 1, \dots, p$. We employ Lasso for (17) in our implementation, and tune the parameter κ_{nj} using tenfold cross-validation, following the usual Lasso literature.

We repeat the above optimization steps iteratively until some stopping criterion is met, e.g., when the estimates in two consecutive iterations are close enough, or when the number of iterations reaches some maximum number. We summarize the above iterative procedure, along with the confidence band derived in the next section, in Algorithm 1.

4 ODE Inference

In this section, we first construct the confidence band for the regulatory effect of $x_k(t)$ on $x_j(t)$ for a given pair $(j, k) \in \{1, \dots, p\}$. We next discuss hypothesis testing for a single pair, then multiple testing for all pairs to reconstruct the entire regulatory system. We also briefly discuss the extension from a single experiment to multiple experiments.

4.1 Confidence band

A confidence band $\mathcal{C}_{n,\alpha}$ is a set of confidence intervals, $\mathcal{C}_{n,\alpha} = \{[c_L(t_0), c_U(t_0)] \mid t_0 \in \mathcal{T}\}$, where $-\infty < c_L(t_0) < c_U(t_0) < \infty$ for any $t_0 \in \mathcal{T}$. Our proposal is built upon but also considerably extends the existing de-biasing methods in high-dimensional inference (Zhang and Zhang, 2014; van de Geer et al., 2014; Ning and Liu, 2017; Zhang and Cheng, 2017; Lu et al., 2020). Our setting is more challenging, as it involves the dynamic ODE system with infinite-dimensional functional object as well as additional measurement error.

First, we propose the following de-biased estimator, given that the functional \tilde{F}_{jk} is

Algorithm 1 Estimation and inference procedure for a given pair $(j, k) \in \{1, \dots, p\}$.

- 1: Initialization with the starting values for $\theta_{jl} = \theta_{jlr} = 1$, $l, r = 1, \dots, p, l \neq k, l \neq r$.
 - 2: Obtain the smoothing spline estimate $\hat{x}_j(t)$ from (6).
 - 3: Obtain the estimate of the global mean $\hat{\theta}_{j0}$ from (8).
 - 4: **repeat**
 - 5: Solve $(\hat{\alpha}_{jk,t_0}, \hat{H}_j)$ in (13) given $\hat{\theta}_j$ through (14) and (16).
 - 6: Solve $\hat{\theta}_j$ in (17) given $(\hat{\alpha}_{j,t}, \hat{H}_t)$ through the Lasso penalized regression (17).
 - 7: **until** the stopping criterion is met.
 - 8: Construct the confidence band by Gaussian multiplier bootstrap from (19).
-

approximated by $\hat{\alpha}_{jk,t_0}$ in our localized kernel learning, to reduce the bias in $\hat{\alpha}_{jk,t_0}$,

$$\hat{F}_{jk}(x_k(t_0)) = \hat{\alpha}_{jk,t_0} + \frac{1}{n} \Sigma_i^\top R_{t_0} \left[(y_j - \bar{y}_j) - \int_{\mathcal{T}} (T_i(t) - \bar{T}(t)) \hat{H}_j(\hat{x}(t)) dt \right], \quad (18)$$

where $\Sigma_i, i = 1, \dots, n$, is the i th row of the $n \times n$ matrix Σ defined in (15), and $\hat{H}_j(\hat{x}(t))$ is obtained from (14). We make a few remarks. First of all, we employ the integral of the infinite-dimensional functional $\hat{H}_j(\hat{x}(t))$ in (18) to correct the bias in $\hat{\alpha}_{jk,t_0}$. As a result, the inference of the de-biased estimator $\hat{F}_{jk}(x_k(t_0))$ relies on analyzing the distribution of the integral, $\int_{\mathcal{T}} \{T_i(t) - \bar{T}(t)\} \hat{H}_j(\hat{x}(t)) dt$, and the measurement error introduced by the estimated trajectory $\hat{x}(t)$. These features clearly differentiate our de-biasing solution from the existing ones. Second, we briefly examine an alternative de-biased estimator that uses the derivative instead of the integral in (18). The convergence of this alternative de-biased estimator hinges on the estimation error of the derivative term, $\mathbb{E} \int_{\mathcal{T}} \{d\hat{x}_j(t)/dt - dx_j(t)/dt\}^2 dt$, which has a slower convergence rate than its integral counterpart (Chen et al., 2017; Dai and Li, 2021). As such, it is to have inferior inference properties, and we choose to use the integral instead of the derivative in our de-biased estimator (18).

Next, we obtain the critical value for the confidence band based on the de-biased estimator (18) using Gaussian multiplier bootstrap. Specifically, we consider the distribution of the supremum of the empirical process, $\sup_{t_0 \in \mathcal{T}} \mathbb{H}_n(t_0)$, where

$$\mathbb{H}_n(t_0) \equiv \sqrt{nh} \left[\hat{F}_{jk}(x_k(t_0)) - F_{jk}(x_k(t_0)) \right], \quad \text{for any } t_0 \in \mathcal{T}.$$

Recognizing that the finite sample distribution of $\mathbb{H}_n(t_0)$ is unknown, we approximate the distribution of $\mathbb{H}_n(t_0)$ by the Gaussian multiplier process (Chernozhukov et al., 2014),

$$\widehat{\mathbb{H}}_n(t_0) \equiv \frac{1}{\sqrt{nh^{-1}}} \sum_{i=1}^n \xi_i \cdot \frac{\widehat{\sigma}_j R_h(t_i - t_0) R_{t_0, i \cdot}^\top \Sigma_k}{\widehat{\sigma}_n(t_0)}, \quad \text{for any } t_0 \in \mathcal{T},$$

where ξ_1, \dots, ξ_n are independent standard normal random variables, the error variance estimator $\widehat{\sigma}_j^2 = \|A_j(y_j - \bar{y}_j) - (y_j - \bar{y}_j)\|^2 / \text{trace}(I_{n \times n} - A_j)$, with $A_j = I_{n \times n} - n\eta_{nj}M_{t_0}^{-1}[I_{n \times n} - \bar{t}(\bar{t}^\top M_{t_0}^{-1}\bar{t})^{-1}\bar{t}^\top M_{t_0}^{-1}] \in \mathbb{R}^{n \times n}$ being the smoothing matrix, and $M_{t_0} = \Sigma R_{t_0}^{-1} + n\eta_{nj}R_{t_0}^{-2} \in \mathbb{R}^{n \times n}$, and $\widehat{\sigma}_n^2(t_0) = n^{-1}\Sigma_k R_{t_0}^2 \Sigma_k$, with the diagonal matrix R_{t_0} defined after (16), and $R_{t_0, i \cdot}, i = 1, \dots, n$, being the i th row of the $n \times n$ matrix R_{t_0} defined in (15). We then compute the critical value for the confidence band as the $(1 - \alpha)$ -quantile of the supremum of the empirical process $\sup_{t_0 \in \mathcal{T}} \widehat{\mathbb{H}}_n(t_0)$ using Gaussian multiplier bootstrap (Giné and Zinn, 1990; Chernozhukov et al., 2014) given the observed data.

Finally, we construct the $100 \times (1 - \alpha)\%$ confidence band for F_{jk} as

$$\mathcal{C}_{n, \alpha} = \left\{ \left[\widehat{F}_{jk}(x_k(t_0)) - \frac{\widehat{c}_n(\alpha)\widehat{\sigma}_n(t_0)}{\sqrt{nh}}, \widehat{F}_{jk}(x_k(t_0)) + \frac{\widehat{c}_n(\alpha)\widehat{\sigma}_n(t_0)}{\sqrt{nh}} \right] \mid t_0 \in \mathcal{T} \right\}, \quad (19)$$

Given the confidence band (19), we can perform hypothesis testing for any given pair $(j, k) \in \{1, \dots, p\}$ and any $t_0 \in \mathcal{T}$ that,

$$H_{0, jk} : x_k(t_0) \text{ has no regulatory effect on } x_j(t_0)$$

$$H_{1, jk} : x_k(t_0) \text{ has nonzero regulatory effect on } x_j(t_0).$$

We use the standardized regulatory effect as the test statistic,

$$z_{jk}(t_0) = \frac{\widehat{F}_{jk}(x_k(t_0))\sqrt{nh}}{\widehat{\sigma}_n(t_0)}, \quad t_0 \in \mathcal{T},$$

which follows the asymptotic distribution $\mathbb{H}_n(t_0)$ under the null hypothesis.

The confidence band (19) is for the inference of the regulatory effect of $x_k(t)$ on $x_j(t)$ for a given pair (j, k) . We can easily couple it with existing multiple testing procedure for *all* pairs of (j, k) to recover the entire regulatory system, e.g., the Benjamini–Hochberg procedure, while controlling the false discovery rate (Benjamini and Hochberg, 1995).

4.2 Extension to multiple experiments

The localized kernel learning method we have developed so far focuses on a single experiment. Meanwhile, it can be easily generalized to incorporate multiple experiments. Specifically, let $\{y_{ij}^{(s)}; i = 1, \dots, n, j = 1, \dots, p, s = 1, \dots, S\}$ denote the observed data from n subjects for p variables under S experiments, with unknown initial conditions $x^{(s)}(0) \in \mathbb{R}^p, s = 1, \dots, S$. Then we modify the localized kernel learning in (10), by seeking $\hat{H}_j \in \mathcal{H}$ and $\hat{\alpha}_{jk,t_0} \in \mathbb{R}$ that minimize

$$\begin{aligned} \frac{1}{Sn} \sum_{s=1}^S \sum_{i=1}^n R_h(t_i - t_0) & \left[\left(y_{ij}^{(s)} - \bar{y}_j^{(s)} \right) - \alpha_{jk,t_0} \bar{t}_i - \int_{\mathcal{T}} (T_i(t) - \bar{T}(t)) H_j(\hat{x}^{(s)}(t)) dt \right]^2 \\ & + \tau_{nj} \left(\sum_{l=1, l \neq k}^p \|\mathcal{P}^l H_j\|_{\mathcal{H}} + \sum_{l=1, l \neq k, r}^p \sum_{r=1, r \neq k}^p \|\mathcal{P}^{lr} H_j\|_{\mathcal{H}} \right), \end{aligned}$$

where $\hat{x}^{(s)}(t) = (\hat{x}_1^{(s)}(t), \dots, \hat{x}_p^{(s)}(t))^{\top}$ is the smoothing spline estimate obtained by,

$$\hat{x}_j^{(s)}(t) = \arg \min_{z_j \in \mathcal{F}} \left\{ \frac{1}{n} \sum_{i=1}^n (y_{ij}^{(s)} - z_j(t_i))^2 + \lambda_{nj} \|z_j(t)\|_{\mathcal{F}}^2 \right\}, \quad j = 1, \dots, p, \quad s = 1, \dots, S.$$

The de-biased estimator in (18) becomes,

$$\hat{F}_{jk}(x_k(t_0)) = \hat{\alpha}_{jk,t_0} + \frac{1}{Sn} \sum_{s=1}^S \Sigma_k^{(s)\top} R_{t_0} \left[\left(y_j^{(s)} - \bar{y}_j^{(s)} \right) - \int_{\mathcal{T}} \{T_i(t) - \bar{T}(t)\} \hat{H}_j(\hat{x}^{(s)}(t)) dt \right].$$

The rest of Algorithm 1 for estimation and inference remains largely the same.

5 Theoretical Properties

In this section, we first establish the rate of convergence for the localized kernel ODE estimator. We then study the asymptotic convergence properties of the constructed confidence band, as well as the recovered regulatory system. Our theoretical results hold for both the low-dimensional setting and the high-dimensional setting, where the number of variables p can be smaller or larger than the sample size n . We also study the regime-switching phenomenon.

5.1 Statistical convergence rate

We begin with three regularity conditions.

Assumption 1. *The kernel density $R(t)$ is a continuous function that has a bounded support, and satisfies that $\int_{\mathcal{T}} R(t)dt = 1$ and $\int_{\mathcal{T}} tR(t)dt = 0$.*

Assumption 2. *The number of nonzero functional components, $\text{card}(\{l : F_{jl} \neq 0\} \cup \{1 \leq l \neq r \leq p : F_{jlr} \neq 0\})$, is bounded, for any $j = 1, \dots, p$.*

Assumption 3. *For any $F_j \in \mathcal{H}$, there exists a random variable B , with $\mathbb{E}(B) < \infty$, and $|\partial F_j(x)/\partial x_k| \leq B\|F_j\|_{L_2}$ almost surely.*

Assumption 1 is standard in the literature on local polynomial regressions (Fan and Gijbels, 1996). Assumption 2 regards the complexity of the functionals. Similar assumptions have been adopted in the sparse additive model over RKHS without interactions (Koltchinskii and Yuan, 2010; Raskutti et al., 2011). Assumption 3 is an inverse Poincaré inequality type condition, which places a regularization on the fluctuation in F_j relative to the L_2 -norm. The same assumption has also been used in additive models in RKHS (Zhu et al., 2014; Dai and Li, 2021).

The next theorem obtains the rate of convergence of our localized kernel estimator.

Theorem 1. *Suppose Assumptions 1 to 3 hold. Suppose $x_j(t) \in \mathcal{F}$, and the RKHS \mathcal{F} is embedded to a β_1 th-order Sobolev space with $\beta_1 > 1/2$. Furthermore, $\tilde{F}_j \in \mathcal{H}$, where \mathcal{H} satisfies (4), and the RKHS \mathcal{H}_l is embedded to a β_2 th-order Sobolev space with $\beta_2 > 1$, $j = 1, \dots, p$, $l = 1, \dots, p$. Then, the localized kernel ODE estimator in (11) satisfies,*

$$\min_{\lambda_{nj} \geq 0} \int_{\mathcal{T}} \left[\hat{F}_j(\hat{x}(t)) - F_j(x(t)) \right]^2 dt = O_p \left(\tau_{nj}^{-\frac{1}{2\beta_2}} \frac{\log n}{nh} + \tau_{nj} + h^{2\beta_2} + \frac{\log p}{n} + n^{-\frac{2\beta_1}{2\beta_1+1}} \right). \quad (20)$$

If $h = O((n/\log n)^{-1/(2\beta_2+2)})$, and $\tau_{nj} = O((n/\log n)^{-\beta_2/(\beta_2+1)})$, then the localized kernel ODE estimator in (11) satisfies that,

$$\min_{\lambda_{nj} \geq 0} \int_{\mathcal{T}} \left[\hat{F}_j(\hat{x}(t)) - F_j(x(t)) \right]^2 dt = O_p \left(\left(\frac{n}{\log n} \right)^{-\frac{\beta_2}{\beta_2+1}} + \frac{\log p}{n} + n^{-\frac{2\beta_1}{2\beta_1+1}} \right). \quad (21)$$

We first examine the sources of the estimation error in (20). There are totally five sources. Specifically, the first source of error $O_p(\tau_{nj}^{-1/2\beta_2} \log n/(np))$ comes from the stochastic error in estimating the interaction terms in the true functional F_j . The second term $O_p(\tau_{nj})$ comes from the bias introduced by using a reproducing kernel method to estimate F_j . The third term $O_p(h^{2\beta_2})$ comes from the localized estimation. The fourth term $O_p(\log p/n)$ comes from the bias introduced by the Lasso estimation. The last term $O_p(n^{-2\beta_1/(2\beta_1+1)})$ comes from the measurement errors in $x(t)$.

We also observe some interesting regime-switching phenomenon in (21). That is, when p is ultrahigh-dimensional, in that $p > \exp[\{n(\log n)^{\beta_2}\}^{1/(\beta_2+1)}]$, then the convergence rate in (21) becomes $O_p(\log p/n + n^{-2\beta_1/(2\beta_1+1)})$. In this case, it matches with the minimax optimal rate for estimating the functional F_j in (3) obtained in Dai and Li (2021). Henceforth, we pay no extra price in terms of the rate of convergence for adopting the localized estimation in this ultrahigh-dimensional setting. On the other hand, when p is low-dimensional, in that $p < \exp[\{n(\log n)^{\beta_2}\}^{1/(\beta_2+1)}]$, then the convergence rate in (21) becomes $O_p((n/\log n)^{-\beta_2/(\beta_2+1)} + n^{-2\beta_1/(2\beta_1+1)})$. Here, the first term $O_p((n/\log n)^{-\beta_2/(\beta_2+1)})$ matches, up to some logarithmic factors, with the rate as if we knew a priori that F_j is an additive model with pairwise interactions. Moreover, the convergence rate $O_p((n/\log n)^{-\beta_2/(\beta_2+1)})$ is slower than the optimal rate $O_p((n/\log n)^{-2\beta_2/(2\beta_2+1)})$ of the kernel ODE estimator of Dai and Li (2021). Such a slower rate is due to the weight matrix R_t introduced by the localized estimation in (10), which increases the variance of estimating F_j by $O_p(h^{-1})$ when compared to the non-localized estimation in Dai and Li (2021). Nevertheless, as we show next, this slower rate is sufficient to establish an asymptotically valid confidence band.

5.2 Coverage properties for the confidence band

A confidence band $\mathcal{C}_{n,\alpha}$ is said to be asymptotically valid with level $100 \times (1 - \alpha)\%$ for F_{jk} , if it satisfies that, for some constants $c, C > 0$,

$$\mathbb{P}(F_{jk}(x(t_0)) \in \mathcal{C}_{n,\alpha}, \forall t_0 \in \mathcal{T}) \geq 1 - \alpha - Cn^{-c}. \quad (22)$$

The condition (22) implies that the confidence band $\mathcal{C}_{n,\alpha}$ has an asymptotic coverage probability at least $1 - \alpha$ for a given data-generating process.

The next theorem establishes the theoretical property of our proposed confidence band $\mathcal{C}_{n,\alpha}$ in (19). We introduce another regularity condition. For any $t \in \mathcal{T}$, let p_j denote the marginal density of $x_j(t)$, p_{jk} denote the bivariate density of $(x_j(t), x_k(t))$, and p_{jkl} denote the joint density of $(x_j(t), x_k(t), x_l(t))$, for $j, k, l = 1, \dots, p$.

Assumption 4. *The density function of $x(t)$ satisfies that,*

$$\sum_{j=1, j \neq k}^p \|p_{jk} - p_j p_k\|_2 \leq \frac{\rho_{\min}}{2B}, \quad \text{and} \quad \sup_{l \neq k} \sum_{j,k=1, j \neq k}^p \|p_{j,k,l} - p_j p_k p_l\|_2 \leq \frac{\rho_{\min}}{2B},$$

for some constant $\rho_{\min} > 0$, and B is as defined in Assumption 3.

Assumption 4 quantifies how weak the dependency between the signal variables can be. Similar conditions have also been used in the inference of the high-dimensional linear regression (Zhang and Zhang, 2014; van de Geer et al., 2014), and the nonparametric additive regression (Lu et al., 2020). We show this condition is also sufficient for establishing the validity of the confidence band in (19) in a complex ODE system.

Theorem 2. *Suppose Assumptions 1 to 4 hold. If $h = O(n^{-r})$, for $r \in (1/5, 3/13)$, then there exist constants $c, C_1 > 0$, such that, for any $\alpha \in (0, 1)$, the confidence band $\mathcal{C}_{n,\alpha}$ in (19) is asymptotically valid.*

Putting all the functionals $\{F_1, \dots, F_p\}$ together forms a network of regulatory relations among the p variables $\{x_1(t), \dots, x_p(t)\}$. The next theorem shows that the estimated system based on our localized kernel ODE approaches the truth with probability tending to one. Denote the set of the true and the estimated regulators of $x_j(t)$ by

$$S_j^* = \{1 \leq k \leq p : F_{jk} \neq 0, \text{ or } F_{jkl} \neq 0 \text{ for some } 1 \leq l \neq k \leq p\},$$

$$\widehat{S}_j = \{1 \leq k \leq p : \widehat{\alpha}_{jk,t_0} \neq 0 \text{ for any } t_0 \in \mathcal{T}\}.$$

We also need two additional regularity conditions. Let $s_j = \text{card}(S_j^*)$. Recall the definitions of $R_{t_0} \in \mathbb{R}^{n \times n}$ in (15), $G \in \mathbb{R}^{n \times (p-1)^2}$ in (17), and the tuning parameter κ_{nj} in (12). Let $G_{S_j^*} \in \mathbb{R}^{n \times s_j}$ denote the sub-matrix of G with the column indices in the set S_j^* .

Assumption 5. *Suppose there exists a constant $C_{\min} > 0$, such that the minimal eigenvalue of the matrix $G_{S_j^*}^\top R_{t_0} G_{S_j^*}$ is no smaller than $C_{\min}/2$. In addition, suppose there exists a constant $0 \leq \xi_G < 1$, such that $\max_{(k,l) \notin S_j^*} \left\| G_{kl}^\top R_{t_0} G_{S_j^*} (G_{S_j^*}^\top R_{t_0} G_{S_j^*})^{-1} \right\|_{L_2} \leq \xi_G$.*

Assumption 6. *Let $\theta_{\min} = \min_{(k,l) \in S_j} \|\theta_{jkl}\|_{L_2}$. Suppose the following inequalities hold for a constant $\eta_{\mathcal{R}} < \infty$:*

$$\frac{\eta_{\mathcal{R}} \sqrt{s_j}}{C_{\min}} + n \kappa_{nj} \frac{\sqrt{s_j}}{C_{\min}} \leq \frac{2}{3} \theta_{\min}, \quad \text{and} \quad \frac{(\xi_G + 1) \sqrt{s_j}}{n \kappa_{nj}} \eta_{\mathcal{R}} + \xi_G \sqrt{s_j} < 1.$$

Assumption 5 ensures the sub-matrix $G_{S_j^*}$ is not degenerated, and the irrelevant variables would not exert too strong an effect on the relevant variables. Assumption 6 imposes some regularity on the minimum effect θ_{\min} , and also characterizes the relationship among ξ_G , κ_{nj} , and s_j . Both assumptions are mild, and similar conditions as Assumptions 5 and 6 have been commonly imposed in the literature (see, e.g., Zhao and Yu, 2006; Meinshausen et al., 2006; Ravikumar et al., 2010; Chen et al., 2017; Dai and Li, 2021).

Theorem 3. *Suppose Assumptions 1, 2, 5 and 6 hold. Then, the localized kernel ODE estimator correctly recovers the true regulatory system, in that,*

$$\mathbb{P} \left(\widehat{S}_j = S_j^* \right) \rightarrow 1, \quad \text{as } n \rightarrow \infty, \quad \text{for all } j = 1, \dots, p.$$

6 Simulation Studies

In this section, we study the finite-sample performance of the confidence band as well as the localized kernel ODE estimator using two well-known ODE systems. In the first example, we focus on the coverage of the confidence band for some given pairs, while in the second example, we study the performance of recovery of the entire regulatory system.

6.1 Enzymatic regulation equations

The first example is a three-node enzyme regulatory system of a negative feedback loop with a buffering node (Ma et al., 2009, NFBLB). The ODE system is given by,

$$\begin{aligned}\frac{dx_1(t)}{dt} &= 10 \frac{x_0\{1 - x_1(t)\}}{\{1 - x_1(t)\} + 0.1} - 10 \frac{x_1(t)}{x_1(t) + 0.1}, \\ \frac{dx_2(t)}{dt} &= 10 \frac{\{1 - x_2(t)\}x_3(t)}{\{1 - x_2(t)\} + 0.1} - 0.2 \frac{x_2(t)}{x_2(t) + 0.1}, \\ \frac{dx_3(t)}{dt} &= 10 \frac{x_1(t)\{1 - x_3(t)\}}{\{1 - x_3(t)\} + 0.1} - 10 \frac{x_2(t)x_3(t)}{x_3(t) + 0.1}.\end{aligned}\tag{23}$$

The input $x_0 \in \mathbb{R}$ is drawn uniformly from $[0.5, 1.5]$, with the initial value $x(0) = 0$. The errors are drawn independently from $\text{Normal}(0, \sigma_j^2)$, with three noise levels, $\sigma_j \in \{0.1, 0.3, 0.5\}$. The time points are evenly distributed, $t_i = (i - 1)/20, i = 1, \dots, n$, with the sample size fixed at $n = 40$. In this example, $p = 3$, and there are $p^2 = 9$ functions in (23) to estimate for each $j = 1, 2, 3$, and in total there are 27 unknown functions.

In this example, we focus on the performance of the confidence band for some given node pairs. Specifically, we examine a nonzero effect $F_{23}(x_3(t))$ that captures the regulatory effect of $x_3(t)$ on $x_2(t)$, and a zero effect $F_{12}(x_2(t))$ of $x_2(t)$ on $x_1(t)$. Correspondingly, we construct the confidence band for $F_{23}(x_3(t))$ and $F_{12}(x_2(t))$, with the 95% significance level, on 500 evenly distributed grid points on $[0, 1]$. In our implementation, we use a first-order Matérn kernel for both steps in (6) and (7) of the collocation method, where $K_{\mathcal{H}_1}(x, x') = (1 + \sqrt{3}\|x - x'\|/\nu) \exp(-\sqrt{3}\|x - x'\|/\nu)$, and ν is chosen by tenfold cross-validation. We have found the results are not overly sensitive to the choice of kernel functions here. We compute the quantile $\hat{c}_n(\alpha)$ in (19) by bootstrap with 500 repetitions.

We note that there is *no* direct competitor to our confidence band solution in the literature. Alternatively, we compare to three commonly used ODE solutions, the linear ODE with interactions (Zhang et al., 2015a), the additive ODE (Chen et al., 2017), and the kernel ODE (Dai and Li, 2021), and couple them with a confidence band that aggregates the point-wise confidence intervals at 500 grid points on $[0, 1]$. For a fair comparison, we

Table 1: The NFBLB example: the empirical coverage probability and area of the confidence band for the varying noise level σ_j . The results are averaged over 500 data replications.

Noise level	Method	Nonzero functional $F_{23}(x_3(t))$		Zero functional $F_{12}(x_2(t))$	
		Coverage probability	Confidence band area	Coverage probability	Confidence band area
$\sigma_j = 0.1$	Linear ODE	0.212	1.550	0.274	2.145
	Additive ODE	0.224	1.332	0.292	2.008
	Kernel ODE	0.939	1.270	0.928	1.848
	Localized kernel ODE	0.974	0.102	0.957	0.217
$\sigma_j = 0.3$	Linear ODE	0.178	1.827	0.224	2.441
	Additive ODE	0.194	1.663	0.262	2.158
	Kernel ODE	0.914	1.381	0.911	1.856
	Localized kernel ODE	0.962	0.163	0.957	0.290
$\sigma_j = 0.5$	Linear ODE	0.123	3.541	0.191	2.538
	Additive ODE	0.141	2.679	0.225	2.350
	Kernel ODE	0.876	1.637	0.902	2.031
	Localized kernel ODE	0.956	0.231	0.948	0.401

adjust the significance level at each of these 500 time points with the Bonferroni correction (Holm, 1979), i.e., $(1 - \alpha/500)\%$, where $\alpha = 0.05$.

We consider two evaluation criteria. One is the empirical coverage probability of the confidence band, and the other is the area of the confidence band, defined as

$$\int_{t_0 \in \mathcal{T}} 2\widehat{c}_n(\alpha)(nh)^{-1/2}\widehat{\sigma}_n(t_0)dt_0,$$

where the integration is computed by discretizing the interval into 1000 grids. A larger coverage probability and a smaller area indicates a better performance.

Table 1 reports the results averaged over 500 data replications. We see that the proposed confidence band achieves the desired coverage for the regulatory effects. In contrast, the confidence bands of the additive and linear ODEs mostly fail to include the truth. This is because there is a discrepancy between the additive and linear ODE model specifications and the true ODE model in (23), and this discrepancy accumulates as the course of the ODE evolves. Meanwhile, the kernel ODE has a much larger confidence band compared to our method. This is because the Bonferroni correction makes the confidence band of kernel ODE overly conservative.

6.2 Lotka-Volterra equations

The second example is the classical Lotka-Volterra system, which consists of pairs of first-order nonlinear differential equations describing the dynamics of biological system in which predators and prey interact (Volterra, 1928). The ODE is given by,

$$\begin{aligned}\frac{dx_{2j-1}(t)}{dt} &= 0.1(2j+11)x_{2j-1}(t) - 0.2(j+1)x_{2j-1}(t)x_{2j}(t), \\ \frac{dx_{2j}(t)}{dt} &= 0.1(2j-1)x_{2j-1}(t)x_{2j}(t) - 0.2(j+1)x_{2j}(t),\end{aligned}\tag{24}$$

for $j = 1, \dots, 5$. Here $dx_{2j-1}(t)/dt$ and $dx_{2j}(t)/dt$ are nonadditive functions of x_{2j-1} and x_{2j} , where x_{2j-1} is the prey and x_{2j} is the predator. The initial values are set as $x_{2j-1}(0) = x_{2j}(0)$. The measurement errors are independent $\text{Normal}(0, \sigma_j^2)$, where the noise level $\sigma_j \in \{1, 2, \dots, 10\}$. The time points are evenly distributed in $[0, 100]$, with $n = 200$. In this example, $p = 10$, and there are $p^2 = 100$ functions in (24) to estimate for each ODE of x_{2j-1} and x_{2j} , $j = 1, \dots, 5$, and in total there are 1000 unknown functions.

In this example, we focus on the performance of recovery of the entire regulatory system through the proposed confidence band coupled with the Benjamini–Hochberg (BH) procedure for multiple testing correction (Benjamini and Hochberg, 1995). Since the ODE equations in (24) only involve the linear and interaction terms, we use the first-order Matérn kernel for the step in (6), and use the linear kernel in (7). As such, the linear and kernel ODEs yield the same estimates. We control the FDR at the level of 20%.

We consider three evaluation criteria, the false discovery proportion, the empirical power, and the trajectory prediction accuracy. The false discovery proportion is defined as the proportion of falsely selected edges in the system out of the total number of edges, and the empirical power is defined as the proportion of selected true edges in the system. We also evaluate the prediction accuracy of the signal trajectory $\hat{F}_j(\hat{x}(t_0))$ as given in (11), by the squared root of the sum of predictive mean squared errors for $x_j(t)$, $j = 1, \dots, 10$, at the unseen “future” time point $t \in [100, 200]$, i.e., $\left\{ \sum_{j=1}^{10} \int_{100}^{200} [\hat{x}_j(t) - x_j(t)]^2 dt \right\}^{1/2}$, where the integral is evaluated at 10000 evenly distributed time points in $[100, 200]$.

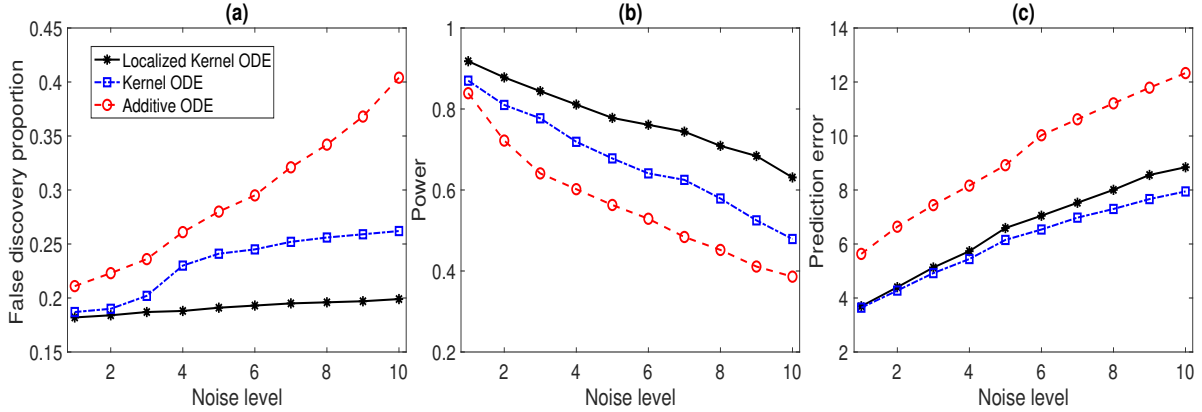


Figure 1: The Lotka-Volterra example: the empirical FDR, power, and trajectory prediction error for the varying noise level σ_j . The results are averaged over 500 data replications.

Figure 1 reports the results averaged over 500 data replications. We see that our method successfully controls the FDR under the nominal level across all noise levels, whereas the additive and kernel ODEs both suffer some inflations, especially when the noise level is high. Meanwhile, our method achieves the best empirical power. In addition, we see that the prediction error of our localized kernel ODE estimator is slightly worse than that of kernel ODE, which agrees with Theorem 1. Nevertheless, this does not affect the inference performance of our method.

7 Data Applications

In this section, we illustrate our method with two data applications, a gene regulatory network analysis given time-course gene expression data, and a brain effective connectivity analysis given electrocorticography (ECoG) data.

7.1 Gene regulatory network

Gene regulation plays a central role in biological activities such as cell growth, development, and response to environmental stimulus. Thanks to the advancement of high-throughput DNA microarray technologies, it becomes feasible to measure the dynamic

Table 2: The gene regulatory network example: the empirical FDR and power for 10 combinations of network structures from GNW. The results are averaged over 500 data replications.

		$p = 10$				$p = 100$			
		Localized kernel ODE	Kernel ODE	Additive ODE	Linear ODE	Localized kernel ODE	Kernel ODE	Additive ODE	Linear ODE
<i>E.coli1</i>	FDR	0.182	0.212	0.241	0.206	0.191	0.194	0.231	0.232
	Power	0.793	0.587	0.547	0.467	0.823	0.611	0.512	0.481
<i>E.coli2</i>	FDR	0.193	0.214	0.332	0.362	0.186	0.201	0.312	0.278
	Power	0.736	0.666	0.639	0.569	0.787	0.684	0.649	0.575
<i>Yeast1</i>	FDR	0.181	0.203	0.214	0.336	0.195	0.193	0.224	0.288
	Power	0.887	0.607	0.546	0.442	0.917	0.642	0.522	0.498
<i>Yeast2</i>	FDR	0.174	0.199	0.262	0.236	0.189	0.211	0.241	0.241
	Power	0.744	0.603	0.570	0.542	0.729	0.582	0.535	0.611
<i>Yeast3</i>	FDR	0.184	0.181	0.189	0.248	0.190	0.208	0.196	0.223
	Power	0.845	0.616	0.573	0.493	0.812	0.577	0.539	0.472

features of gene expression profiles on a genome scale. Such time-course gene expression data allow investigators to study gene regulatory networks, and ODE modeling is frequently employed for such a purpose (Lu et al., 2011). The data we analyze is the in silico benchmark gene expression data generated by GeneNetWeaver (GNW) using dynamical models of gene regulations and nonlinear ODEs (Schaffter et al., 2011). GNW extracts two regulatory networks of *E.coli*, *E.coli1*, *E.coli2*, and three regulatory networks of yeast, *yeast1*, *yeast2*, *yeast3*, each of which has two dimensions, $p = 10$ nodes and $p = 100$ nodes. The system of ODEs for each extracted network is based on a thermodynamic approach, and the resulting ODE system is non-additive and nonlinear (Marbach et al., 2010). For the 10-node network, GNW provides $S = 4$ perturbation experiments, and for the 100-node network, GNW provides $S = 46$ experiments. In each perturbation experiment, GNW generates the time-course data with different initial conditions of the ODE system to emulate the diversity of gene expression trajectories (Marbach et al., 2009). All the trajectories are measured at $n = 21$ evenly spaced time points in $[0, 1]$. We add independent measurement errors from $\text{Normal}(0, 0.025^2)$, which is the same as the DREAM3 competition and the data analysis in Henderson and Michailidis (2014).

We apply the proposed confidence band approach, coupled with the BH procedure

at the 20% FDR level, to this data. Table 2 reports the area under the ROC curve for the recovered regulatory network for all ten combinations of network structures, and the results are averaged over 100 data replications. We compare with the alternative methods of linear, additive, and kernel ODEs, similarly as in Section 6.1. We see clearly that the proposed method performs competitively in all cases. This example also shows that the proposed method can scale up and work with reasonably large networks. For instance, for the network with $p = 100$ nodes, there are $p^2 = 10,000$ functions to estimate.

7.2 Brain effective connectivity analysis

Brain effective connectivity refers explicitly to the directional influence that one neural system exerts over another (Friston, 2011), and is of central interest in neuroscience research. Effective connectivity analysis uncovers such directional influences among different brain regions through imaging techniques such as electrocorticographic (ECoG), and modeling techniques such as ODE (Zhang et al., 2015a). The data we analyze is an ECoG study of the brain during decision making (Saez et al., 2018). It consists of the ECoG recordings of $p = 61$ electrodes placed in the orbitofrontal cortex (OFC) region of an epilepsy patient when performing gambling tasks with different levels of winning risk. The patient performed 72 rounds of gambling games in total, half of which are low-risk games, and half are high-risk games. We analyze the low-risk and high-risk games separately, with $S = 36$. The length of the ECoG signals for each round of game is $n = 3001$. See Saez et al. (2018) for more details about the data collection and processing.

We again apply the proposed confidence band approach, coupled with the BH procedure at the 20% FDR level, to this data. To identify the nodes that show different connectivity patterns under two risk groups, we focus on those nodes whose total number of inward and outward edges is no more than 2 in one risk type, but no fewer than 9 in the other risk type. This results in node 1 that is located in the cytoarchitectural region of OFC called Fo2, node 4 located in Fo3, and node 54 located in Fo1 (Henssen et al., 2016).

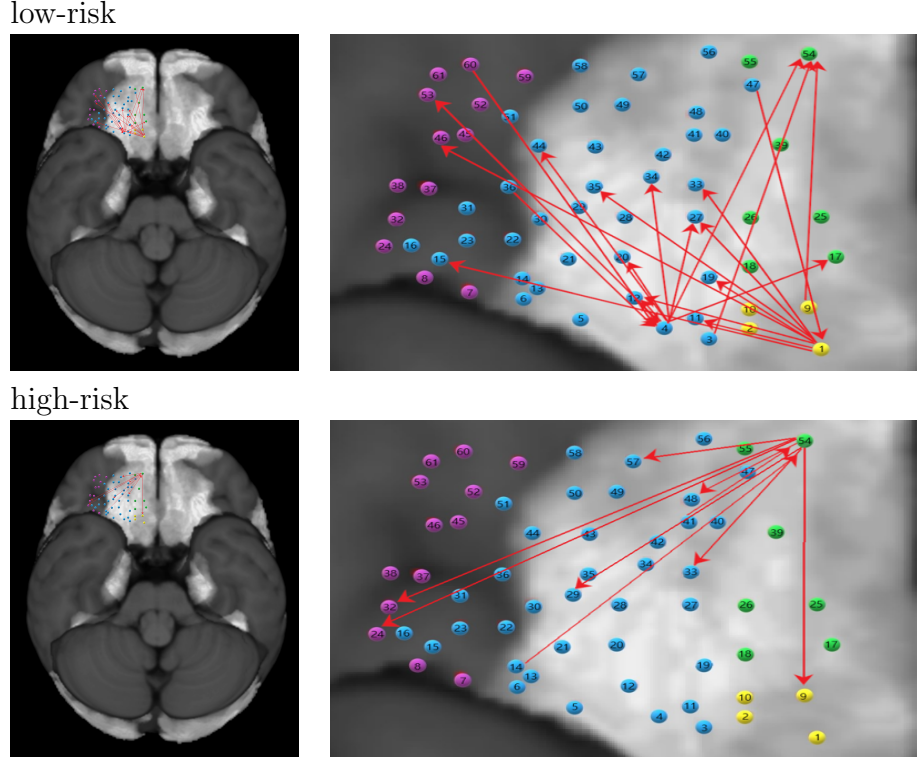


Figure 2: The brain effective connectivity example: the connectivity patterns during the low-risk and high-risk games. The colored nodes correspond to different cytoarchitectural regions of orbitofrontal cortex. Green: Fo1; yellow: Fo2; blue: Fo3; purple: other regions. The left panels are for the entire brain, and the right panels for the enlarged areas.

Figure 2 plots the estimated connectivity patterns of these three nodes, first on the entire brain, then in an amplified area. We see that, for nodes 1 and 4, there are many more outward edges during the low-risk games than the high-risk games, whereas for node 54, there are many more outward edges during the high-risk games than the low-risk games. Note that both Fo2 and Fo3 belong to the posterior OFC, which is more involved in simple reward type decision making, whereas Fo1 belongs to the anterior OFC, which is involved in abstract reward (Kringelbach and Rolls, 2004). Our results suggest that the posterior OFC is more active during the low-risk games, in which the reward is relatively simple and clear. Meanwhile, the anterior OFC tends to more actively influence other nodes during the high-risk games, which involve more calculations and harder decisions.

References

- Aronszajn, N. (1950). Theory of reproducing kernels. *Transactions of the American Mathematical Society*, 68:337–404.
- Benjamini, Y. and Hochberg, Y. (1995). Controlling the false discovery rate: a practical and powerful approach to multiple testing. *Journal of the Royal statistical society: series B (Methodological)*, 57(1):289–300.
- Cao, J. and Zhao, H. (2008). Estimating dynamic models for gene regulation networks. *Bioinformatics*, 24:1619–1624.
- Cao, X., Sandstede, B., and Luo, X. (2019). A functional data method for causal dynamic network modeling of task-related fmri. *Frontiers in Neuroscience*, 13:127.
- Chen, S., Shojaie, A., and Witten, D. M. (2017). Network reconstruction from high-dimensional ordinary differential equations. *Journal of the American Statistical Association*, 112:1697–1707.
- Chernozhukov, V., Chetverikov, D., and Kato, K. (2014). Anti-concentration and honest, adaptive confidence bands. *Annals of Statistics*, 42(5):1787–1818.
- Dai, X. and Li, L. (2021). Kernel ordinary differential equations. *Journal of the American Statistical Association*, pages 1–35.
- Dattner, I. and Klaassen, C. A. J. (2015). Optimal rate of direct estimators in systems of ordinary differential equations linear in functions of the parameters. *Electronic Journal of Statistics*, 9:1939–1973.
- Fan, J. and Gijbels, I. (1996). *Local Polynomial Modelling and Its Applications*. Monographs on Statistics and Applied Probability (Vol. 66), London: Chapman & Hall.

- Friston, K. J. (2011). Functional and effective connectivity: A review. *Brain Connectivity*, 1(1):13–36.
- Giné, E. and Zinn, J. (1990). Bootstrapping general empirical measures. *The Annals of Probability*, pages 851–869.
- González, J., Vujačić, I., and Wit, E. (2014). Reproducing kernel hilbert space based estimation of systems of ordinary differential equations. *Pattern Recognition Letters*, 45:26–32.
- Gu, C. (2013). *Smoothing Spline ANOVA Models*. Springer Science & Business Media.
- Henderson, J. and Michailidis, G. (2014). Network reconstruction using nonparametric additive ode models. *PLOS ONE*, 9:1–15.
- Henssen, A., Zilles, K., Palomero-Gallagher, N., Schleicher, A., Mohlberg, H., Gerboga, F., Eickhoff, S. B., Bludau, S., and Amunts, K. (2016). Cytoarchitecture and probability maps of the human medial orbitofrontal cortex. *Cortex*, 75:87–112.
- Holm, S. (1979). A simple sequentially rejective multiple test procedure. *Scandinavian journal of statistics*, pages 65–70.
- Huang, J. Z. (1998). Projection estimation in multiple regression with application to functional anova models. *Annals of Statistics*, 26(1):242–272.
- Izhikevich, E. (2007). *Dynamical Systems In Neuroscience*. MIT Press.
- Koltchinskii, V. and Yuan, M. (2010). Sparsity in multiple kernel learning. *Annals of Statistics*, 38:3660–3695.
- Kringelbach, M. L. and Rolls, E. T. (2004). The functional neuroanatomy of the human orbitofrontal cortex: evidence from neuroimaging and neuropsychology. *Progress in Neurobiology*, 72(5):341–372.

- Liang, H. and Wu, H. (2008). Parameter estimation for differential equation models using a framework of measurement error in regression models. *Journal of the American Statistical Association*, 103:1570–1583.
- Lin, Y. and Zhang, H. H. (2006). Component selection and smoothing in multivariate nonparametric regression. *Annals of Statistics*, 34:2272–2297.
- Lu, J., Kolar, M., and Liu, H. (2020). Kernel meets sieve: Post-regularization confidence bands for sparse additive model. *Journal of the American Statistical Association*, 115(532):2084–2099.
- Lu, T., Liang, H., Li, H., and Wu, H. (2011). High-dimensional ODEs coupled with mixed-effects modeling techniques for dynamic gene regulatory network identification. *Journal of the American Statistical Association*, 106:1242–1258.
- Ma, W., Trusina, A., El-Samad, H., Lim, W. A., and Tang, C. (2009). Defining network topologies that can achieve biochemical adaptation. *Cell*, 138:760–773.
- Marbach, D., Prill, R. J., Schaffter, T., Mattiussi, C., Floreano, D., and Stolovitzky, G. (2010). Revealing strengths and weaknesses of methods for gene network inference. *Proceedings of the National Academy of Sciences*, 107:6286–6291.
- Marbach, D., Schaffter, T., Mattiussi, C., and Floreano, D. (2009). Generating realistic in silico gene networks for performance assessment of reverse engineering methods. *Journal of Computational Biology*, 16:229–239.
- Meinshausen, N., Bühlmann, P., et al. (2006). High-dimensional graphs and variable selection with the lasso. *Annals of Statistics*, 34(3):1436–1462.
- Miao, H., Wu, H., and Xue, H. (2014). Generalized ordinary differential equation models. *Journal of the American Statistical Association*, 109(508):1672–1682.

- Mikkelsen, F. V. and Hansen, N. R. (2017). Learning large scale ordinary differential equation systems. *arXiv preprint arXiv:1710.09308*.
- Ning, Y. and Liu, H. (2017). A general theory of hypothesis tests and confidence regions for sparse high dimensional models. *The Annals of Statistics*, 45(1):158 – 195.
- Opsomer, J. D. and Ruppert, D. (1997). Fitting a bivariate additive model by local polynomial regression. *Annals of Statistics*, 25:186–211.
- Ramsay, J. O., Hooker, G., Campbell, D., and Cao, J. (2007). Parameter estimation for differential equations: a generalized smoothing approach. *Journal of the Royal Statistical Society. Series B (Statistical Methodology)*, 69:741–796.
- Raskutti, G., Wainwright, M. J., and Yu, B. (2011). Minimax rates of estimation for high-dimensional linear regression over ℓ_q -balls. *IEEE Transactions on Information Theory*, 57:6976–6994.
- Ravikumar, P., Wainwright, M. J., and Lafferty, J. (2010). High-dimensional ising model selection using l_1 -regularized logistic regression. *Annals of Statistics*, 38:1287–1319.
- Saez, I., Lin, J., Stolk, A., Chang, E., Parvizi, J., Schalk, G., Knight, R. T., and Hsu, M. (2018). Encoding of multiple reward-related computations in transient and sustained high-frequency activity in human ofc. *Current Biology*, 28(18):2889–2899.
- Schaffter, T., Marbach, D., and Floreano, D. (2011). Genenetweaver: in silico benchmark generation and performance profiling of network inference methods. *Bioinformatics*, 27:2263–2270.
- van de Geer, S., Bühlmann, P., Ritov, Y. A., and Dezeure, R. (2014). On asymptotically optimal confidence regions and tests for high-dimensional models. *Annals of Statistics*, 42:1166–1202.

- Varah, J. M. (1982). A spline least squares method for numerical parameter estimation in differential equations. *SIAM Journal on Scientific and Statistical Computing*, 3:28–46.
- Volterra, V. (1928). Variations and Fluctuations of the Number of Individuals in Animal Species living together. *ICES Journal of Marine Science*, 3:3–51.
- Wahba, G. (1990). *Spline Models for Observational Data*. SIAM, Philadelphia.
- Wahba, G., Wang, Y., Gu, C., Klein, R., and Klein, B. (1995). Smoothing spline ANOVA for exponential families, with application to the Wisconsin Epidemiological Study of Diabetic Retinopathy. *Annals of Statistics*, 23:1865–1895.
- Wansbeek, T. and Meijer, E. (2001). Measurement error and latent variables. *A Companion to Theoretical Econometrics*. Oxford: Basil Blackwell, pages 162–179.
- Wu, H., Lu, T., Xue, H., and Liang, H. (2014). Sparse additive ordinary differential equations for dynamic gene regulatory network modeling. *Journal of the American Statistical Association*, 109:700–716.
- Wu, L., Qiu, X., Yuan, Y.-x., and Wu, H. (2019). Parameter estimation and variable selection for big systems of linear ordinary differential equations: a matrix-based approach. *Journal of the American Statistical Association*, 114(526):657–667.
- Zhang, C.-H. and Zhang, S. S. (2014). Confidence intervals for low dimensional parameters in high dimensional linear models. *Journal of the Royal Statistical Society. Series B.*, 76(1):217–242.
- Zhang, T., Wu, J., Li, F., Caffo, B., and Boatman-Reich, D. (2015a). A dynamic directional model for effective brain connectivity using electrocorticographic (ECoG) time series. *Journal of the American Statistical Association*, 110:93–106.

- Zhang, T., Yin, Q., Caffo, B., Sun, Y., and Boatman-Reich, D. (2017). Bayesian inference of high-dimensional, cluster-structured ordinary differential equation models with applications to brain connectivity studies. *Annals of Applied Statistics*, 11:868–897.
- Zhang, X., Cao, J., and Carroll, R. J. (2015b). On the selection of ordinary differential equation models with application to predator-prey dynamical models. *Biometrics*, 71(1):131–138.
- Zhang, X. and Cheng, G. (2017). Simultaneous inference for high-dimensional linear models. *Journal of the American Statistical Association*, 112(518):757–768.
- Zhao, P. and Yu, B. (2006). On model selection consistency of lasso. *Journal of Machine Learning Research*, 7:2541–2563.
- Zhu, H., Yao, F., and Zhang, H. H. (2014). Structured functional additive regression in reproducing kernel hilbert spaces. *Journal of the Royal Statistical Society. Series B (Statistical Methodology)*, 76:581–603.